Coherent Control of Isotope Separation in HD^+ Photodissociation by Strong Fields

Eric Charron,[1] Annick Giusti-Suzor,[1,2] and Frederick H. Mies[3]

[1]*Laboratoire de Photophysique Moléculaire, Université Paris-Sud, 91405 Orsay, France*
[2]*Laboratoire de Chimie-Physique, 11 rue Pierre et Marie Curie, 75231 Paris, France*
[3]*National Institute of Standards and Technology, Gaithersburg, Maryland 20899*
(Received 5 January 1995)

The photodissociation of the HD^+ molecular ion in intense short-pulsed linearly polarized laser fields is studied using a time-dependent wave-packet approach where molecular rotation is fully included. We show that applying a coherent superposition of the fundamental radiation with its second harmonic can lead to asymmetries in the fragment angular distributions, with significant differences between the hydrogen and deuterium distributions in the long wavelength domain where the permanent dipole is most efficient. This effect is used to induce an appreciable isotope separation.

PACS numbers: 33.80.Gj, 33.80.Wz

Control of chemical reactivity using two-color laser fields has been actively investigated in the past few years. The use of a coherent superposition of a fundamental radiation with one of its harmonics can induce complex interference effects between different pathways in atomic or molecular processes [1]. This method is shown here to be a useful tool to control molecular dissociation in the high intensity regime. Although several interesting processes have been discovered (above threshold dissociation [2,3], bond softening [3,4], and vibrational trapping [5–7]), they are generally in competition and are not easily disentangled in practice. This experimental fact motivated us to determine laser parameters that will specifically enhance one of these physical processes. Indeed, we have shown that in intense laser fields the branching ratios of H_2^+ in the different photodissociation channels can be appreciably controlled in a $(\omega, 3\omega)$ experiment [8] and that asymmetric angular distributions of the fragments H^+ and $H(1s)$ can be created in a $(\omega, 2\omega)$ experiment [9]. Encouraged by the efficiency of this method, we decided to explore possible asymmetries in the photodissociation of HD^+.

This ion presents an asymmetric electronic distribution that is small in the bound molecule but becomes extremely important when the fragments dissociate. This is because the two lowest electronic states, of $^2\Sigma^+$ symmetry, asymptotically lead to either $H^+ + D(1s)$ or $H(1s) + D^+$, with an energy difference of 29.8 cm^{-1}, which is due to the larger reduced mass of the electron on the deuterium compared to the hydrogen atom [10,11]. In the ground state, the electron is localized near the deuterium atom while for the first excited state it is on the hydrogen. The chemical difference between these two dissociative channels together with the inherent simplicity of this system makes HD^+ one of the best candidates for demonstrating laser-induced control of chemical reactivity.

To simulate the dissociation of the HD^+ molecular ion subjected to an intense and short laser pulse, we solve the time-dependent Schrödinger equation using the short-time propagator splitting method [12]. The molecular ion

interacts with a classical linearly polarized electric field made by a coherent superposition of a fundamental radiation of angular frequency ω_f and electric field amplitude E_f with its second harmonic of angular frequency $\omega_h = 2\omega_f$ and amplitude E_h

$$\mathbf{E}(t) = f(t)\{E_f\cos(\omega_f t) + E_h\cos(\omega_h t + \varphi)\}\hat{\mathbf{e}}, \quad (1)$$

where $f(t) = \sin^2(\pi t/2T_p)$ is a Gaussian-like pulse shape of width T_p and total duration $2T_p$. The wave function describing HD^+ is restricted to include only the two first electronic states, with $\phi_G(\mathbf{r}, R)$ and $\phi_E(\mathbf{r}, R)$ denoting their electronic wave functions

$$\Phi(\mathbf{R}, \mathbf{r}, t) = \{F_G(\mathbf{R}, t)\phi_G + F_E(\mathbf{R}, t)\phi_E\}\chi_s. \quad (2)$$

$\mathbf{R} = (R, \theta_R, \phi_R)$ is the internuclear vector joining the hydrogen to the deuterium, and $\mathbf{r}$ is the electronic coordinate. The electron spin, described by the χ_s function of space-fixed projections $s = \pm 1/2$, acts here as a spectator and is uncoupled from the molecular frame. $F_G(\mathbf{R}, t)$ and $F_E(\mathbf{R}, t)$ denote the time-dependent nuclear wave functions associated with each electronic state and contain nuclear dynamic information.

To introduce the angular degrees of freedom of the molecule, we expand each nuclear wave function in a large basis set of spherical harmonics $Y_{N,M}(\theta_R, \phi_R)$ (typically 20 to 40 angular momenta N are necessary to achieve convergence [7], depending on the field intensity). We assume HD^+ to be initially ($t = 0$) in a well defined rovibrational level (v_0, N_0, M_0) of the ground electronic state: $F_G(\mathbf{R}, 0) = \psi_{v_0,N_0}(R)Y_{N_0,M_0}(\theta_R, \phi_R)$ and $F_E(\mathbf{R}, 0) = 0$. For a linearly polarized electric field the initial M_0 quantum number is conserved, and the wave functions $F_G(\mathbf{R}, t)$ and $F_E(\mathbf{R}, t)$ are expanded on a set of spherical harmonics with fixed azimuthal quantum number

$$F_{G(E)}(\mathbf{R}, t) = \sum_N F_{G(E),N}(R, t)Y_{N,M_0}(\theta_R, \phi_R). \quad (3)$$

In contrast to the H_2^+ case [9], this expansion in the spherical harmonics basis includes both parities for each

electronic state, due to the *permanent dipole moment* in HD^+, which allows transitions within a given electronic state. Indeed, the radiative interaction directly couples the nuclear wave functions of components $N \leftrightarrow N \pm 1$. The corresponding coupling matrix elements, evaluated in the length gauge, take the same form as for H_2^+

$$V_{N,N-1}^{\alpha\beta}(R,t) = \mu_{\alpha\beta}(R)\sqrt{\frac{N^2 - M_0^2}{(2N-1)(2N+1)}}\, E(t),$$

(4)

except for the expression of the different dipole moments $\mu_{\alpha\beta}(R)$ between a pair of electronic states denoted by the subscripts α and $\beta \equiv G$ or E. To take the nondegeneracy effects into account, and thus present the correct dissociation behavior, we use the *transformed* Hamiltonian defined by Moss and Sadler [10], and employ the *coupled states* approach of Carrington and co-workers [11]. We expand the resultant ground ϕ_G and first excited ϕ_E electronic wave functions in terms of the pure $1s\sigma_g$ and $2p\sigma_u$ solutions of the Born-Oppenheimer Hamiltonian

$$\phi_G = a(R)\phi_{1s\sigma_g} + b(R)\phi_{2p\sigma_u} \underset{R\to\infty}{\sim} +\phi_{1s}(D),$$

$$\phi_E = -b(R)\phi_{1s\sigma_g} + a(R)\phi_{2p\sigma_u} \underset{R\to\infty}{\sim} -\phi_{1s}(H),$$

(5)

where $a \simeq 1$ and $b \simeq 0$ for short internuclear distances. At large distances, both a and b approach $1/\sqrt{2}$ and the ϕ_G and ϕ_E wave functions correlate with the $1s$ atomic orbitals centered on the deuteron or on the proton, respectively. On the way to dissociation, the electron can no more "jump" from one fragment to the other, and the electronic dipole moment $\mu_{EG}(R)$ vanishes at long distance. But in this limit, the internal couplings $\mu_{GG}(R)$ and $\mu_{EE}(R)$ diverge as $-2R/3$ and $R/3$, respectively [10,11]. The nonadiabatic couplings induced by the nondiagonal elements of the $\partial^2/\partial R^2$ kinetic energy operator in the (G,E) electronic basis are also included in the time propagation using an additional basis transformation.

At the end of the propagation, the partial nuclear wave functions $F_{G(E),N}(R,t=2T_p)$ are projected on the corresponding field-free continuum nuclear wave functions to get the dissociation probabilities. One thus obtains the energetic and angular distributions of the fragments [9], to be compared with experimental data when available.

A simplified four-state model can be derived from the above multistate treatment in analogy with the two-state model commonly used for the H_2^+ ion in intense laser fields [5,8] if one assumes that the molecular ion is totally aligned by the laser electric field along its polarization axis. This alignment has been demonstrated experimentally by different groups [13] and results from the optical pumping of the rotational quantum number N [9]. To take the effect of the permanent dipole moments $\mu_{GG}(R)$ and $\mu_{EE}(R)$ into account, we associate *two* nuclear wave packets with each electronic potential, representing the collective sum of the *odd* (o) and the *even* (e) partial wave components in Eq. (3). The total

wave function in Eq. (2) can then be expressed simply as follows:

$$\Phi = \{(F_{G,o} + F_{G,e})\phi_G + (F_{E,o} + F_{E,e})\phi_E\}\chi_s.$$

(6)

We propagate an initial ($t = 0$) wave packet taken as a pure v_0 vibrational state of the ground electronic potential. The $\mu_{GG}(R)$, $\mu_{EE}(R)$, and $\mu_{EG}(R)$ dipole moments are included in the potential matrix as off-diagonal terms that couple nuclear wave functions of opposite parity. This simple model saves a lot of time and memory in computation and has been checked to give reliable results. The angular distribution of the H^+ fragment can be obtained from the projections $C_{G,o}(\varepsilon)$ and $C_{G,e}(\varepsilon)$ of the odd and even G nuclear wave packets at the end of the pulse on the G field-free continuum nuclear wave function at the energy ε by

$$P_{H^+}(\varepsilon, \theta = 0°) = \tfrac{1}{2}|C_{G,o}(\varepsilon) - C_{G,e}(\varepsilon)|^2,$$

$$P_{H^+}(\varepsilon, \theta = 180°) = \tfrac{1}{2}|C_{G,o}(\varepsilon) + C_{G,e}(\varepsilon)|^2,$$

(7)

where $\theta = 0°$ and $\theta = 180°$ denote the *forward* and *backward* ion signals [8,9]. The directional dissociation probabilities are obtained by energy integration

$$P_{H^+}(\theta = 0° \text{ or } 180°) = \int P_{H^+}(\varepsilon, \theta = 0° \text{ or } 180°)\, d\varepsilon,$$

(8)

and the total dissociation probability P_{H^+} in the ground electronic state is just the sum of these two directional probabilities. Similar equations [with opposite signs in Eq. (7)] relative to the excited part E of the wave packet give the partial and total productions of D^+ ions.

The most remarkable effect on the angular distributions of the HD^+ photofragments is obtained using a coherent superposition of the second (or any even) harmonic with a fundamental laser frequency. In this case a given energy of dissociation ε can be reached by absorbing *odd* as well as *even* numbers of photons. Thus, for example, $C_{G,o}(\varepsilon)$ and $C_{G,e}(\varepsilon)$ can simultaneously contribute to the probabilities in Eq. (7), and the cross term $\mathrm{Re}\{C_{G,o}^*(\varepsilon)C_{G,e}(\varepsilon)\}$ induces different dissociation probabilities in the $\theta = 0°$ and $\theta = 180°$ directions. This effect is similar to the asymmetric angular distributions of photoelectrons observed in two-color high intensity atomic photoionization [14], or to the asymmetric proton angular distributions in H_2^+ photodissociation [9]. However, what is unique here is that we can also induce different asymmetries in the distributions of the H^+ and D^+ photofragments and control the spatial separation of these isotopes. This effect requires long wavelength lasers, such as the CO_2 laser case shown in Fig. 1 using $\lambda_f = 10.6$ μm ($\hbar\omega_f = 970$ cm^{-1}) and $\lambda_h = 5.3$ μm ($\hbar\omega_h = 1940$ cm^{-1}).

This figure presents the fully converged 3D results obtained from an expansion using up to 40 coupled partial waves in each electronic potential [see Eq. (3)], for an initial ($v_0 = 0$, $N_0 = 0$, $M_0 = 0$) rovibrational state and

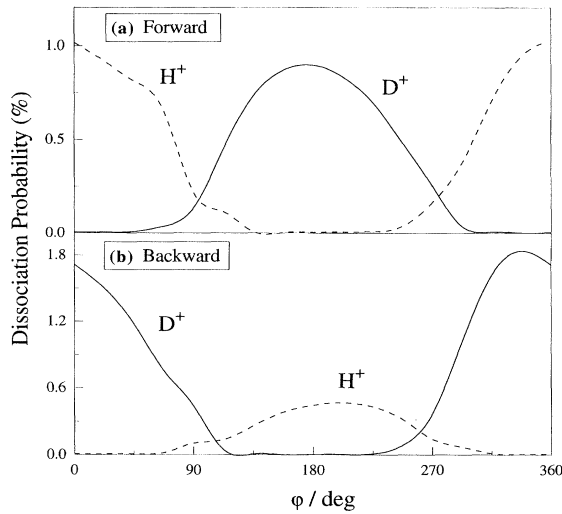FIG. 1. Dissociation probabilities of HD^+ in the two first electronic states leading to the $H^+ + D(1s)$ (dashed line) and $H(1s) + D^+$ (solid line) fragments as a function of the phase shift φ between the two laser harmonics. The integrated forward ($\theta \approx 0°$) probabilities are shown in (a), and the integrated backward ($\theta \approx 180°$) probabilities are shown in (b), for a laser pulse of 225 fs duration made by the coherent superposition of the two wavelengths $\lambda_f = 10.6$ μm and $\lambda_h = 5.3$ μm with the intensities $I_f = 5 \times 10^{13}$ W cm^{-2} and $I_h = 2 \times 10^{13}$ W cm^{-2}. The HD^+ molecular ion is initially in the ($v_0 = 0$, $N_0 = 0$, $M_0 = 0$) rovibrational state.

using peak intensities $I_f = 5 \times 10^{13}$ W cm^{-2} and $I_h = 2 \times 10^{13}$ W cm^{-2} to evaluate the electric fields in Eq. (1). The pulse duration is 225 fs, corresponding to 13 optical cycles of the second harmonic. For each chosen phase φ the *forward* and *backward* dissociation probabilities for a particular fragment are obtained by angular integration of the 3D distributions over $0° \le \theta \le 90°$ and $90° \le \theta \le 180°$, respectively, where θ denotes the angle between the dissociation and the polarization axis.

The polar plot in Fig. 2 for the specific phase $\varphi = 0$ confirms that the angular distributions are closely peaked along the polarization axis $\hat{e}$. For this phase shift $\varphi = 0$, essentially 100% of the dissociated ions emitted in the
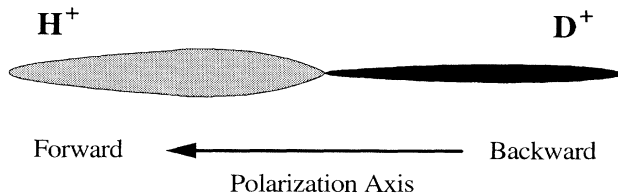

FIG. 2. Polar plot showing the angular distributions of the H^+ and D^+ ions with the same conditions as in Fig. 1 for the specific phase $\varphi = 0$. Note the better alignment of D^+, due to a more efficient rotational pumping [9] in the excited electronic state.

forward direction are expected to be H^+, and the D^+ ions are almost only ejected in the *backward* direction. Obviously, this gives a very efficient mechanism for spatially separating the isotopes.

In this dissociation scheme, a neutral atom $H(1s)$ or $D(1s)$ always appears in the opposite direction to the other ion (D^+ or H^+). A significant ionization of the neutral atoms on the way to the detector should thus just enhance the ion signal, and increase the efficiency of the separation process. If the phase shift is changed to $\varphi = \pi$ the direction of ejection of the H^+ and D^+ ions is simply reversed, due to a change in the sign of the cross term in Eq. (7). It is just near $\varphi = \pi/2$ that the isotopes are not separated.

The explorations we have made show that this separation effect is robust enough to survive experimental uncertainties in the intensities of both harmonics and in their phases. Increasing the pulse length from 225 to 675 fs has a negligible effect on the angular asymmetry for $\varphi = 0$. We further tested the experimental feasibility by performing the same calculations for a wide range of initial vibrational and rotational states and found the same qualitative behavior as in Fig. 1 for $v_0 = 0, 1, 2, 3$ and $N_0 = 0, 1, 2$ and $M_0 = 0, \pm 1$. This coherent control should thus persist even after averaging over an initial distribution of the HD^+ states, as expected in a real experiment.

The most sensitive parameter for achieving coherent control of the isotope separation in HD^+ photodissociation is the laser frequency ω_f in Eq. (1). Indeed, twice the CO_2 laser photon energy (1940 cm^{-1}) is comparable to the vibrational spacing in the HD^+ ground electronic state. A choice of laser frequency in this range greatly enhances the efficiency of the $\mu_{GG}(R)$ and $\mu_{EE}(R)$ permanent transition dipoles. The variations of the *forward* and *backward* dissociation probabilities as a function of the fundamental wavelength used in this two-color study are shown in Fig. 3 for the most favorable phase $\varphi = 0$. These 1D calculations are presented for the initial level $v_0 = 3$ using the same intensities as in Fig. 1. The remarkable separability seen in Fig. 2 persists over the full range of frequencies $500 \le \hbar\omega_f \le 2500$ cm^{-1}.

It is interesting to note that there are two distinct regions of enhanced probability of photodissociation in Fig. 3, which we interpret as low and high frequency mechanisms. The first one is analogous to the static field *tunneling regime* found in strong field photoionization and photodissociation [15], while the second is closer to the Floquet *multiphoton regime*. The long wavelength (low frequency) mechanism, where appreciable dissociation occurs during a single optical cycle [15], favors the spatial separation of the isotopes. In this regime, pathways induced by the permanent dipoles μ_{GG} and μ_{EE}, which have *opposite* signs, manifest interferences with those due to the μ_{EG} transition dipole, and it allows us to achieve this remarkable control. On the contrary, the fragmentation dynamics in the short wavelength (high frequency) domain
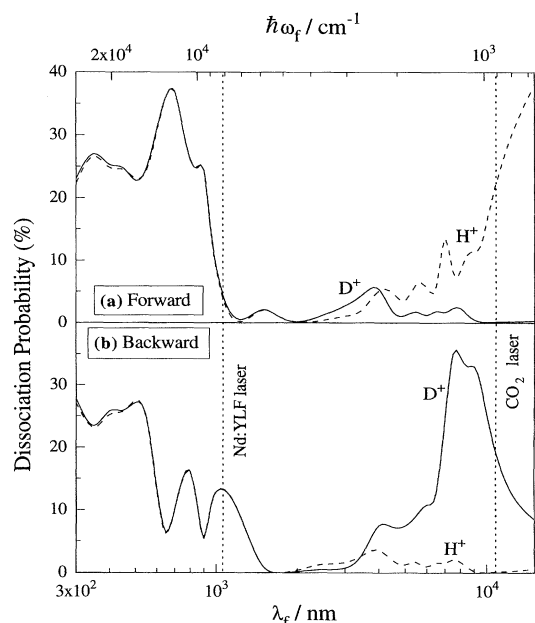
FIG. 3. 1D-dissociation probabilities of HD^+ ($v_0 = 3$) in the forward (a) and backward (b) directions leading to the $H^+ + D(1s)$ (dashed line) and $H(1s) + D^+$ (solid line) fragments as a function of the fundamental wavelength. The phase of the second harmonic is fixed to $\varphi = 0$. The pulse duration and laser intensities are the same as in Fig. 1.

is characterized by two features that destroy this interference effect. First, because nothing significant happens during one optical period, the dissociation dynamics reflects behavior "averaged" over the optical cycle. Second, unfavorable Franck-Condon factors between nuclear wave functions differing by the energy of one photon within a given electronic state reduce the effect of permanent dipoles. In fact, since the μ_{EG} coupling dominates the dissociation in this high frequency limit, the dynamics of HD^+ is very similar to the one of H_2^+ and no appreciable difference between the H^+ and D^+ partial probabilities can be induced in this regime, as observed by Sheehy, Walker, and DiMauro [16].

In this paper we have predicted a new and efficient mechanism for separating different isotopic products in a fragmentation process. Unlike previous examples of coherent control that only controlled the distribution of all the charged particles together, we are now able to distinguish the fragments of different masses. This scenario should extend far beyond the specific example of HD^+ and can be applied to separating products of a different chemical nature as well. Tailoring quantum interferences induced by two-color coherent light opens a promising avenue for controlling the dynamics of quasisymmetric systems, and applications of primary importance can be expected in enantio-differentiation, for instance [17].

[1] M. Shapiro, J. W. Hepburn, and P. Brumer, Chem. Phys. Lett. **149**, 451 (1988).

[2] A. Giusti-Suzor, X. He, O. Atabek, and F. H. Mies, Phys. Rev. Lett. **64**, 515 (1990).

[3] P. H. Bucksbaum, A. Zavriyev, H. B. Muller, and D. W. Schumacher, Phys. Rev. Lett. **64**, 1883 (1990); A. Zavriyev, P. H. Bucksbaum, H. B. Muller, and D. W. Schumacher, Phys. Rev. A **42**, 5500 (1990); B. Yang, M. Saeed, L. F. DiMauro, A. Zavriyev, and P. H. Bucksbaum, Phys. Rev. A **44**, R1458 (1991).

[4] G. Jolicard and O. Atabek, Phys. Rev. A **46**, 5845 (1992).

[5] A. Giusti-Suzor and F. H. Mies, Phys. Rev. Lett. **68**, 3869 (1992); G. Yao and S. I. Chu, Chem. Phys. Lett. **197**, 413 (1992); Phys. Rev. A **48**, 485 (1993).

[6] A. Zavriyev, P. H. Bucksbaum, J. Squier, and F. Saline, Phys. Rev. Lett. **70**, 1077 (1993).

[7] E. E. Aubanel, J. M. Gauthier, and A. D. Bandrauk, Phys. Rev. A **48**, 2145 (1993); E. E. Aubanel, A. Conjusteau, and A. D. Bandrauk, Phys. Rev. A **48**, R4011 (1993).

[8] E. Charron, A. Giusti-Suzor, and F. H. Mies, Phys. Rev. Lett. **71**, 692 (1993).

[9] E. Charron, A. Giusti-Suzor, and F. H. Mies, Phys. Rev. A **49**, R641 (1994).

[10] R. E. Moss and I. A. Sadler, Mol. Phys. **61**, 905 (1987); **66**, 591 (1989).

[11] A. Carrington and R. A. Kennedy, Mol. Phys. **56**, 935 (1985); A. Carrington, I. R. McNab, and C. A. Montgomerie, J. Phys. B **22**, 3551 (1989).

[12] M. J. Feit, J. A. Fleck, and A. Steiger, J. Comput. Phys. **47**, 412 (1982).

[13] D. Normand, L. A. Lompré, and C. Cornaggia, J. Phys. B **25**, L497 (1992); D. T. Strickland, Y. Beaudoin, P. Dietrich, and P. B. Corkum, Phys. Rev. Lett. **68**, 2755 (1992).

[14] H. G. Muller, P. H. Bucksbaum, D. W. Schumacher, and A. Zavriyev, J. Phys. B **23**, 2761 (1990); Y. Y. Yin, C. Chen, and D. S. Elliott, Phys. Rev. Lett. **69**, 2353 (1992); K. J. Shafer and K. C. Kulander, Phys. Rev. A **45**, 8026 (1992); D. W. Schumacher, F. Weihe, H. G. Muller, and P. H. Bucksbaum, Phys. Rev. Lett. **73**, 1344 (1994).

[15] P. Dietrich and P. B. Corkum, J. Chem. Phys. **97**, 3187 (1992).

[16] B. Sheehy, B. Walker, and L. DiMauro, Phys. Rev. Lett. **74**, 4799 (1995).

[17] P. Brumer and M. Shapiro, Sci. Am. **272**, No. 3, 34 (1995).